# ON GEOMETRICALLY SELF-SIMILAR MODES IN WALL-BOUNDED TURBULENT FLOWS

**Rashad Moarref**
Graduate Aerospace Laboratories
California Institute of Technology
Pasadena, CA 91125, USA
rashad@caltech.edu

**Ati S. Sharma**
Engineering and the Environment
University of Southampton
Southampton, SO17 1BJ, United Kingdom
a.sharma@soton.ac.uk

**Joel A. Tropp**
Computing & Mathematical Sciences
California Institute of Technology
Pasadena, CA 91125, USA
jtropp@cms.caltech.edu

**Beverley J. McKeon**
Graduate Aerospace Laboratories
California Institute of Technology
Pasadena, CA 91125, USA
mckeon@caltech.edu

## ABSTRACT

A gain-based low-rank approximation (McKeon & Sharma, 2010) of the Navier-Stokes equations is utilized to describe the possibility of geometrically self-similar modes in the overlap region of wall-bounded turbulent flows. We establish that a necessary condition for existence of self-similar velocity fluctuations is the presence of a logarithmic turbulent mean velocity. Under the practical assumption that the mean velocity consists of a logarithmic region, we identify the scalings that constitute hierarchies of self-similar modes. It is shown that the elements of a hierarchy are parameterized by the critical wall-normal location where the speed of the mode equals the local turbulent mean velocity: The height and width of the modes scale linearly and the length of the modes scales quadratically with the critical wall-normal location.

## INTRODUCTION

Wall turbulence is an attractive area of research owing to its tremendous scientific and technological implications. It is characterized by a broad range of spatial scales ranging from large energetic eddies with outer length scales (e.g. the boundary layer thickness) to small energetic and dissipative eddies with viscous length scales (i.e. the ratio between kinematic viscosity and wall shear velocity). The gap between the outer and viscous eddy scales is bridged by an overlap region where the size of the energetic eddies is believed to be proportional to their distance from the wall. Notwithstanding many important advances in understanding these scalings, a unifying theory of turbulence is still lacking.

One of the most successful theories that mechanistically describes the turbulent mean velocity and fluctuation intensities relies on the attached-eddy hypothesis (Townsend, 1976). Townsend hypothesized that the overlap region is occupied by a forest of geometrically self-similar attached eddies. These eddies are attached in the sense that their height scales with their distance from the wall, and they are self-similar since their wall-parallel length scales are proportional to their height. This model systematically predicts that if the population density of the attached eddies inversely decreases with their height, both the turbulent mean velocity and the wall-parallel energy intensities exhibit logarithmic dependence with the distance from the wall (Perry & Chong, 1982). These predictions were recently confirmed using high-Reynolds number experiments (Marusic *et al.*, 2013). However, the attached eddy hypothesis does not predict the exact shape of the eddies or their evolution in time.

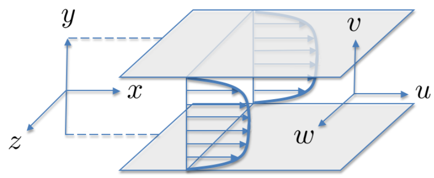


Figure 1. Pressure driven channel flow.

Our objective is to investigate the self-similar modes in the logarithmic region using the Navier-Stokes equations (NSE). The geometric similarity of the optimal transient response to initial perturbations and the optimal responses to harmonic and stochastic forcings was highlighted by Hwang & Cossu (2010) using the linearized NSE with turbulent eddy viscosity. These authors found that the streamwise constant optimal responses scale with the spanwise wavelength in the wall-normal direction for spanwise wavelengths in the overlap region.

In the present study, we argue that the self-similar modes are inherent features of the NSE in the presence of a logarithmic mean velocity. This is done by establishing that hierarchies of geometrically self-similar velocity fields are admitted by a rank-1 model (in the wall-normal direction) based on the principal response modes of the resolvent operator at each wall-parallel wavenumbers and frequencies.

## MODEL OVERVIEW

We provide an overview of a low-rank approximation to turbulent channel flow following the development of McKeon & Sharma (2010) for pipe configuration.

### Decomposition in the homogeneous directions

The velocity is decomposed into the Fourier modes in the homogeneous wall-parallel directions and time

$$
\begin{aligned}
\mathbf{u}(x,y,z,t) \; = \\
\iiint_{-\infty}^{\infty} \hat{\mathbf{u}}(y;\kappa_x,\kappa_z,\omega)\,\mathrm{e}^{\mathrm{i}(\kappa_x x+\kappa_z z-\omega t)}\mathrm{d}\kappa_x\,\mathrm{d}\kappa_z\,\mathrm{d}\omega,
\end{aligned}
\tag{1}
$$

where $\mathbf{u}(x,y,z,t) = [u\ v\ w]^T$ is the velocity vector, $x$ and $z$ are the infinitely long streamwise and spanwise directions, $0 \le y \le 2$ is the wall-normal direction (see figure 1 for the geometry), $t$ is time, $\hat{}$ denotes a variable in the transformed domain, $\kappa_x$ and $\kappa_z$ are the streamwise and spanwise wavenumbers, and $\omega$ is the temporal (angular) frequency. For any $(\kappa_x,\kappa_z,\omega)\neq 0$, $\hat{\mathbf{u}}(y;\kappa_x,\kappa_z,\omega)$ represents a propagating wave with streamwise and spanwise wavelengths $\lambda_x = 2\pi/\kappa_x$ and $\lambda_z = 2\pi/\kappa_z$ and streamwise speed $c = \omega/\kappa_x$.

An equation for velocity fluctuations $\hat{\mathbf{u}}(y;\kappa_x,\kappa_z,\omega)$ around the turbulent mean velocity, $\mathbf{U}(y) = [U(y)\ 0\ 0]^T = \hat{\mathbf{u}}(y;0,0,0)$, is given by

$$
\begin{aligned}
-\mathrm{i}\omega\hat{\mathbf{u}} + (\mathbf{U}\cdot\nabla)\hat{\mathbf{u}} + (\hat{\mathbf{u}}\cdot\nabla)\mathbf{U} + \nabla\hat{p} - (1/Re_\tau)\Delta\hat{\mathbf{u}} \;&=\; \hat{\mathbf{f}},\\
\nabla\cdot\hat{\mathbf{u}} \;&=\; 0.
\end{aligned}
\tag{2}
$$

Here, $\mathbf{f} = [f_1\ f_2\ f_3]^T = -(\mathbf{u}\cdot\nabla)\mathbf{u}$ is the convective nonlinearity in the NSE, $p$ is the pressure, $\nabla = [\mathrm{i}\kappa_x\ \partial_y\ \mathrm{i}\kappa_z]^T$ is the gradient, and $\Delta = \partial_{yy} - \kappa^2$ with $\kappa^2 = \kappa_x^2 + \kappa_z^2$ is the Laplacian. The Reynolds number $Re_\tau = u_\tau h/\nu$ is defined based on the channel half-height $h$, kinematic viscosity $\nu$, and friction velocity $u_\tau = \sqrt{\tau_w/\rho}$, where $\tau_w$ is the shear stress at the wall, and $\rho$ is the density. Velocity is normalized by $u_\tau$, spatial variables by $h$, time by $h/u_\tau$, and pressure by $\rho u_\tau^2$. The spatial variables are denoted by $^+$ when normalized by the viscous length scale $\nu/u_\tau$, e.g. $y^+ = Re_\tau y$. In the present study, the turbulent mean velocity is an *a priori*-known parameter in the model. However, notice that the velocity fluctuations in the full model sustain the mean velocity.

### Decomposition in the wall-normal direction

The input-output relationship between $\hat{\mathbf{f}}$ and $\hat{\mathbf{u}}$ in (2) is given by

$$
\begin{aligned}
\hat{\mathbf{u}}(y;\kappa_x,\kappa_z,\omega) \;&=\; H(\kappa_x,\kappa_z,\omega)\,\hat{\mathbf{f}}(y;\kappa_x,\kappa_z,\omega),\\
H(\kappa_x,\kappa_z,\omega) \;&=\; C(\kappa_x,\kappa_z)R(\kappa_x,\kappa_z,\omega)C^\dagger(\kappa_x,\kappa_z),
\end{aligned}
\tag{3}
$$

where $H(\kappa_x,\kappa_z,\omega)$ is the transfer function from $\hat{\mathbf{f}}$ to $\hat{\mathbf{u}}$, cf. figure 2, the resolvent operator $R(\kappa_x,\kappa_z,\omega)$ is the transfer function for the system with the wall-normal velocity/vorticity states, the operator $C$ is mapping the wall-normal velocity/vorticity to $\hat{\mathbf{u}}$, and $C^\dagger$ is the adjoint of $C$.

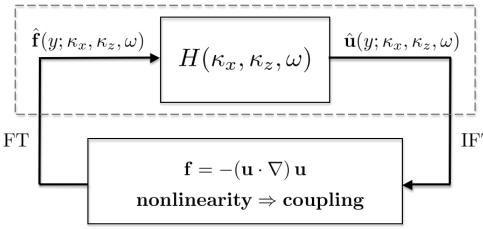


Figure 2. For any triplet $(\kappa_x,\kappa_z,\omega)$, the operator $H(\kappa_x,\kappa_z,\omega)$ maps the forcing $\hat{\mathbf{f}}$ to the response $\hat{\mathbf{u}}$. The different wavenumbers are coupled via the quadratic relationship between $\mathbf{f}(x,y,z,t)$ and $\mathbf{u}(x,y,z,t)$. FT and IFT stand for Fourier transform and inverse Fourier transform, respectively. The input-output map (shown with the dashed rectangle) is the main focus of the present study.

These operators are given by

$$
\begin{aligned}
R \;&=\; \begin{bmatrix} R_1 & 0 \\ \mathrm{i}\kappa_z U' & R_2 \end{bmatrix}^{-1}, \quad C \;=\; \frac{1}{\kappa^2}\begin{bmatrix} \mathrm{i}\kappa_x\partial_y & -\mathrm{i}\kappa_z \\ \kappa^2 & 0 \\ \mathrm{i}\kappa_z\partial_y & \mathrm{i}\kappa_x \end{bmatrix},\\
C^\dagger \;&=\; \begin{bmatrix} -\mathrm{i}\kappa_x\Delta^{-1}\partial_y & \kappa^2\Delta^{-1} & -\mathrm{i}\kappa_z\Delta^{-1}\partial_y \\ \mathrm{i}\kappa_z & 0 & -\mathrm{i}\kappa_x \end{bmatrix},\\
R_1 \;&=\; \Delta^{-1}\left(\mathrm{i}\kappa_x((U-c)\Delta - U'') - (1/Re_\tau)\Delta^2\right),\\
R_2 \;&=\; \mathrm{i}\kappa_x(U-c) - (1/Re_\tau)\Delta,
\end{aligned}
\tag{4}
$$

where $\Delta^2 = \partial_{yyyy} - 2\kappa^2\partial_{yy} + \kappa^4$, and prime denotes differentiation in $y$, e.g. $U'(y) = \mathrm{d}U/\mathrm{d}y$. As illustrated in figure 2, each transfer function represents a linear sub-unit of the full NSE. In addition, the nonlinear terms wrap a feedback-loop around the linear sub-units and act as a forcing term that drives the velocity fluctuations.

A gain-based wall-normal basis is determined using the Schmidt (singular value) decomposition of $H(\kappa_x,\kappa_z,\omega)$

$$
\begin{aligned}
\hat{\mathbf{u}}(y;\kappa_x,\kappa_z,\omega) \;&=\; H(\kappa_x,\kappa_z,\omega)\,\hat{\mathbf{f}}(y;\kappa_x,\kappa_z,\omega) \;= \\
&\sum_{j=1}^{\infty} a_j(\kappa_x,\kappa_z,\omega)\,\sigma_j(\kappa_x,\kappa_z,\omega)\,\hat{\psi}_j(y;\kappa_x,\kappa_z,\omega),\\
a_j(\kappa_x,\kappa_z,\omega) \;&=\; \int_{-1}^{1}\hat{\phi}_j^*(y;\kappa_x,\kappa_z,\omega)\,\hat{\mathbf{f}}(y;\kappa_x,\kappa_z,\omega)\,\mathrm{d}y,
\end{aligned}
\tag{5}
$$

where $\sigma_1 \ge \sigma_2 \ge \cdots > 0$ denote the singular values of $H$, and the singular functions $\hat{\phi}_j = [\hat{f}_{1j}\ \hat{f}_{2j}\ \hat{f}_{3j}]^T$ and $\hat{\psi}_j = [\hat{u}_j\ \hat{v}_j\ \hat{w}_j]^T$ are respectively the forcing and response directions corresponding to $\sigma_j$ and satisfy an orthonormality constraint

$$
\begin{aligned}
\int_{-1}^{1}\hat{\phi}_j^*(y;\kappa_x,\kappa_z,\omega)\,\hat{\phi}_k(y;\kappa_x,\kappa_z,\omega)\,\mathrm{d}y \;&=\; \delta_{jk},\\
\int_{-1}^{1}\hat{\psi}_j^*(y;\kappa_x,\kappa_z,\omega)\,\hat{\psi}_k(y;\kappa_x,\kappa_z,\omega)\,\mathrm{d}y \;&=\; \delta_{jk},
\end{aligned}
\tag{6}
$$

where $\delta$ denotes the Kronecker delta. The computational approach and the necessary treatments for obtaining unique singular functions are detailed in Moarref *et al.* (2013).

### The rank-1 approximation

It follows from the singular value decomposition (5) that if the forcing is aligned in the $\hat{\phi}_j$ direction with unit energy, the response is aligned in the $\hat{\psi}_j$ direction with energy $\sigma_j^2$. Following Moarref *et al.* (2013), a rank-1 model is obtained by only keeping the principal singular directions in the wall-normal coordinate for any wall-parallel wavenumbers and frequencies. This is motivated by the observation that the operator $H$ acts as a directional amplifier (see, for example, McKeon & Sharma, 2010). Several results in wall turbulence were obtained using the rank-1 approximation, see e.g. McKeon *et al.* (2013). To decouple analyses of the nonlinear forcing and the linear sub-units, we consider an unstructured forcing in the wall-parallel directions and time.

## NECESSARY CONDITIONS FOR EXISTENCE OF SELF-SIMILAR MODES

The modal decomposition of the velocity field facilitates analysis of the contribution of different modes with parameters $(\kappa_x, \kappa_z, c)$ to the total velocity. The definitive role of wave speed $c$ in determining the universal (invariant with Reynolds number) scales of turbulent channels was emphasized in Moarref *et al.* (2013). In the rest of the paper, the modes are characterized by $c$ instead of $\omega$ and we note that, for a given $\kappa_x$, prescribing either $c$ or $\omega$ yields the other one. In this section, we determine the necessary conditions for the presence of geometrically self-similar modes, over a range of $(\kappa_x, \kappa_z, c)$, consistent with the dynamics of the linear sub-units in the NSE described by $H(\kappa_x, \kappa_z, c)$.

### First condition: Logarithmic shape of the mean velocity

Self-similarity of the principal singular functions of $H$ relies on scalability of $H$ in the spatial directions. Since the resolvent operator contains $y$-dependent coefficients, i.e. $U(y) - c$ and its wall-normal derivatives $U'(y)$ and $U''(y)$, cf. (4), scalability of $H$ in $y$ requires scalability of the above coefficients. This reduces to identifying the necessary conditions under which

$$U(y) - c \;=\; g_1(y/y_c), \qquad (7)$$

for some functions $U(y)$ and $g_1(y)$ and some scale $y_c$ to be determined. Let the relationship between $c$ and $y_c$ be governed by $c = g_2(y_c)$. Then, we seek the functions $U$, $g_1$, $g_2$, and the scale $y_c$ such that

$$U(y) \,-\, g_2(y_c) \;=\; g_1(y/y_c). \qquad (8)$$

It follows from (8) that $g_2(y) = U(y) - g_1(1)$, $g_1(y) = U(y) - g_2(1)$, and $g_2(1) = U(1) - g_1(1)$. Therefore, (8) can be rewritten as $U(y) - \big(U(y_c) - g_1(1)\big) \;=\; U(y/y_c) - \big(U(1) - g_1(1)\big)$, or $U(y) - U(y_c) = U(y/y_c) - U(1)$. The only functions that satisfy this constraint are the constant function and the logarithmic function and we have

$$U(y) \;=\; d_1 + d_2 \log_{d_3}(y), \quad c \;=\; U(d_4 y_c), \qquad (9)$$

where $d_1$ to $d_4$ are constants. The wall-normal scale corresponds to the wall-normal location where $c = U(d_4 y_c)$. The constant $d_4$ is arbitrary since it enters as a coefficient in front of the scale $y_c$. We select $d_4 = 1$ such that $y_c$ is the critical wall-normal location corresponding to the wave speed $c$.

There is an abundance of numerical and experimental evidence that support the presence of a logarithmic turbulent mean velocity (see, for a recent summary, Smits *et al.*, 2011)

$$U \;=\; B + (1/\kappa)\log(y^+), \;\; y_l \le y \le y_u. \qquad (10)$$

Here, $B$ is an additive constant, $\kappa$ is the von Kármán's constant, and $y_l$ and $y_u$ are respectively the lower and upper bounds of the logarithmic region. The constants in (9) are obtained upon direct comparison with (10).

### Second condition: Locality of the singular functions of $H$

The boundary conditions in the finite direction $y$ and the wall-normal symmetry relative to the center plane pose limitations on wall-normal scaling of the resolvent. These limitations can be removed if the singular functions have a zero support near the walls and the center plane. Moarref *et al.* (2013) showed that the singular functions corresponding to the energetically significant modes are in fact localized. This was explained by the observation that the peak of the principal singular functions occurs at or near the critical wall-normal location where $U(y) - c$ is locally minimized for a given wave speed (McKeon & Sharma, 2010).

We consider $y_l^+ = 100$ and $y_u = 0.1$ for the bounds of the 'logarithmic' region to exclude the truly inner and outer regions of the turbulent mean velocity, and note that recent experiments suggest that the lower bound on the logarithmic region depends on the Reynolds number: $y_l^+ \sim Re_\tau^{1/2}$, see Marusic *et al.* (2013). Owing to the locality of the singular functions around the critical layer, the modes with speeds in the 'logarithmic' region, $c_l \le c \le c_u$, are at least one decade away from the walls and the center plane and the boundary effects are negligible. Here, $c_l$ and $c_u$ are given by $c_l = U(y_l^+ = 100) = 16$, and $c_u = U(y_u = 0.1) = U_{cl} - 6.15$, with $U_{cl}$ denoting the centerline velocity.

### Third condition: Balance between viscous dissipation and mean advection terms

The scalings in the wall-parallel directions follow from the balance between the viscous dissipation term, $(1/Re_\tau)\Delta$, and the mean advection terms, e.g. $\mathrm{i}\kappa_x(U - c)$, in the resolvent, cf. $R_1$ and $R_2$ in (4). The self-similarity requires scaling of the spanwise wavelength with $y_c$ and the streamwise wavelength with $y_c^+ y_c$,

$$\bar{\lambda}_x = \lambda_x/(y_c^+ y_c), \;\; \bar{y} \,=\, y/y_c, \;\; \bar{\lambda}_z = \lambda_z/y_c. \qquad (11)$$

The differential operators in $y$ and the wall-normal wavenumbers in the $y_c$-scaled coordinates are given by $\partial/\partial_{\bar{y}} = y_c(\partial/\partial_y), \bar{\kappa}_x = (y_c^+ y_c)\kappa_x, \bar{\kappa}_z = y_c\kappa_z$. For given $\bar{\kappa}_x$ and $\bar{\kappa}_z$, the Laplacian, $\Delta = y_c^{-2}(\partial_{\bar{y}\bar{y}} - (y_c^+)^{-2}(\bar{\kappa}_x)^2 - (\bar{\kappa}_z)^2)$, approximately scales with $y_c^{-2}$ if $(\bar{\kappa}_z)^2$ dominates $(y_c^+)^{-2}(\bar{\kappa}_x)^2$, i.e.

$$\kappa_z/\kappa_x \;=\; \lambda_x/\lambda_z \;=\; y_c^+ (\bar{\lambda}_x/\bar{\lambda}_z) \;\gtrsim\; \gamma. \qquad (12)$$

We consider a conservative value of $\sqrt{10}$ for the threshold $\gamma$ and note that this value can be modified. This agrees

Table 1. Summary of the self-similar scalings in the logarithmic region of the turbulent mean velocity. The growth/decay rates that these scales induce on the principal singular value and the principal singular functions of $H$ are shown. The critical wall-normal location corresponding to the wave speed is denoted by $y_c$, i.e. $c = U(y_c)$.

| $\lambda_x$ | $y$ | $\lambda_z$ | $\sigma_1$ | $u_1$ | $v_1, w_1$ |
|---|---|---|---|---|---|
| $y_c^+ y_c$ | $y_c$ | $y_c$ | $\left(y_c^+\right)^2 y_c$ | $y_c^{-1/2}$ | $\left(y_c^+\right)^{-1} y_c^{-1/2}$ |

with the observation of Hwang & Cossu (2010) that the optimal responses were approximately similar for $\kappa_x \ll \kappa_z$. Since the aspect ratio $\lambda_x/\lambda_z$ increases with $y_c^+$, the smallest value of $y_c^+$ for which (12) is guaranteed is equal to $y_{c_1}^+ = \gamma(\bar{\lambda}_z/\bar{\lambda}_x)$. Therefore, the smallest wave speed that satisfies the aspect ratio constraint and lies in the logarithmic region is given by

$$c_1 \;=\; \max\left(16,\, B + (1/\kappa)\log y_{c_1}^+\right). \tag{13}$$

Then, the operators $R$, $C$, and $C^\dagger$ in (4) scale as

$$\begin{aligned}
R &= \begin{bmatrix} (y_c^+ y_c)\bar{R}_1 & 0 \\ (y_c^+)^2 \bar{R}_3 & (y_c^+ y_c)\bar{R}_2 \end{bmatrix}, \\
C &= \begin{bmatrix} (1/y_c^+)\bar{C}_1 & (y_c)\bar{C}_2 \\ \bar{C}_3 & 0 \\ \bar{C}_4 & (1/Re_\tau)\bar{C}_5 \end{bmatrix}, \\
C^\dagger &= \begin{bmatrix} (1/y_c^+)\bar{C}_1^\dagger & \bar{C}_3^\dagger & \bar{C}_4^\dagger \\ (1/y_c)\bar{C}_2^\dagger & 0 & \left(y_c^+ y_c\right)^{-1}\bar{C}_5^\dagger \end{bmatrix}.
\end{aligned} \tag{14}$$

For given $\bar{\kappa}_x$ and $\bar{\kappa}_z$ that satisfy the constraint (12), the operators $\bar{C}_1$ to $\bar{C}_5$ and their adjoints are approximately independent of $y_c$ and $Re_\tau$. In addition, the operators $\bar{R}_1$ to $\bar{R}_3$ are approximately independent of $y_c$ and $Re_\tau$ when acting on functions whose supports are localized, cf. the above-mentioned locality condition. From (14), we have

$$H = \begin{bmatrix} (y_c^+ y_c)\bar{H}_{11} & (y_c^+)^2 (y_c)\bar{H}_{12} & (y_c^+)^2 (y_c)\bar{H}_{13} \\ (y_c)\bar{H}_{21} & (y_c^+ y_c)\bar{H}_{22} & (y_c^+ y_c)\bar{H}_{23} \\ (y_c)\bar{H}_{31} & (y_c^+ y_c)\bar{H}_{32} & (y_c^+ y_c)\bar{H}_{33} \end{bmatrix}, \tag{15}$$

where the operators $\bar{H}_{ij}$ are effectively independent of $y_c$ and $Re_\tau$ when acting on their principal singular functions. Since $y_c^+ \geq y_l^+ = 100$, the principal singular value of $H$ is proportional to $(y_c^+)^2 y_c$. In addition, the orthonormality constraints (6) on $\hat{\psi}_1$ and $\hat{\phi}_1$ require that $u_1$ scales with $y_c^{-1/2}$. This is because the supports of $\hat{\psi}_1$ and $\hat{\phi}_1$ expand with $y_c$. Furthermore, $v_1$ and $w_1$ scale with $(y_c^+)^{-1} y_c^{-1/2}$.

## THE SELF-SIMILAR MODES

Upon satisfaction of the above-mentioned conditions, the principal singular functions of $H$ yield hierarchies of geometrically self-similar modes that are uniquely parameterized by the critical wall-normal distance $y_c$, i.e. $c = U(y_c)$. As summarized in table 1, the height and width of the self-similar modes scale with $y_c$ and their length with $y_c^+ y_c$. Any hierarchy is a subset of wave parameters and can be described by a representative mode with $\lambda_{x,r}$, $\lambda_{z,r}$, and $c_r = U(y_{c_r})$ that belongs the hierarchy.

The isosurfaces of streamwise velocity associated with three modes that belong to the hierarchy with $\kappa_{x,r} = 1$, $\kappa_{z,r} = 10$, and $c_r = (2/3)U_{cl}$ are shown in figure 3(a). The larger modes propagate faster and lean more towards the wall since the length of the modes grows quadratically with the height. The vertical cross-sections of the streamwise velocity for these three modes at $x = 0$ and $z = 0$ are shown in figures 3(b) and 3(c). As the wave speed increases, the peaks of the modes move away from the wall, see figures 3(b) and 3(c). In addition, the modes are attached in the sense of Townsend since they have energetic legs that reach down to the wall and their heights scale with $y$.

The loci of wave parameters that belong to three demonstrative hierarchies with representative modes marked by open circles are shown in figure 4(a) for $Re_\tau = 10000$. The mode with $\kappa_{x,r} = 1$, $\kappa_{z,r} = 10$, and $c_r = (2/3)U_{cl}$ (black) was shown to be representative of the very large-scale motions (McKeon & Sharma, 2010). The representative modes for the other hierarchies have the same wavenumbers but different speeds, i.e. $c_r = 16$ (blue) and $U_{cl} - 6.15$ (red), corresponding to the mean velocity at the lower and upper bounds of the 'logarithmic' region. Each locus constitutes a vertical line after normalizing the length and width of the modes according to the scales in table 1 obtained from the resolvent. In fact, the singular functions of $H$ are self-similar along any vertical line as long as $\lambda_x/\lambda_z \gtrsim \gamma$. The aspect ratio constraint requires that the wave parameters lie above the shaded threshold plane $\lambda_x/\lambda_z = \gamma$ in figure 4(a). For example, the modes corresponding to the dashed segment of the hierarchy with $c_r = U_{cl} - 6.15$ do not belong to any hierarchy.

Owing to the self-similarity, the principal singular values and singular functions of $H$ for all the modes in a given hierarchy can be determined from its representative mode. The principal singular value $\sigma_1$ corresponding to the modes that belong to the hierarchies in figure 4(a) are shown in figure 4(b). The singular values grow with $(y_c^+)^2 y_c$ as theoretically predicted, cf. table 1. Figure 4(c) shows the principal streamwise singular function $u_1$ corresponding to the hierarchy with $\kappa_{x,r} = 1$, $\kappa_{z,r} = 10$, and $c_r = (2/3)U_{cl}$ for $100/Re_\tau \leq y_c \leq 0.1$. The arrow shows the direction of increasing $y_c$. Normalizing and scaling the singular functions according to table 1 collapses the singular functions for different wave speeds, see black curves in figure 4(d).

Figure 4(d) also shows the scaled singular functions corresponding to the hierarchies with $\kappa_{x,r} = 1$, $\kappa_{z,r} = 10$, and $c_r = 16$ (blue) and $U_{cl} - 6.15$ (red). We see that the normalized and scaled singular functions lie on the top of each other for the hierarchy with $c_r = 16$. For the hierarchy with $c_r = U_{cl} - 6.15$, the singular functions for large $y_c$ collapse on each other while the singular functions for small $y_c$ are considerably different. This is expected since the aspect ratios of the modes fall below $\gamma$ as $y_c$ decreases, i.e. for this hierarchy, the modes corresponding to small $y_c$ lie below the shaded threshold plane in figure 4(a).

Figures 4(e)-4(j) show similar curves to those in figure 4(d) for the wall-normal and spanwise velocity components. Notice that the self-similarity is weaker for the velocity components that are less localized in the wall-normal direction. For example, the self-similarity is lost as the bulk of the spanwise mode moves outside the upper edge of the logarithmic region for large values of $y_c$.

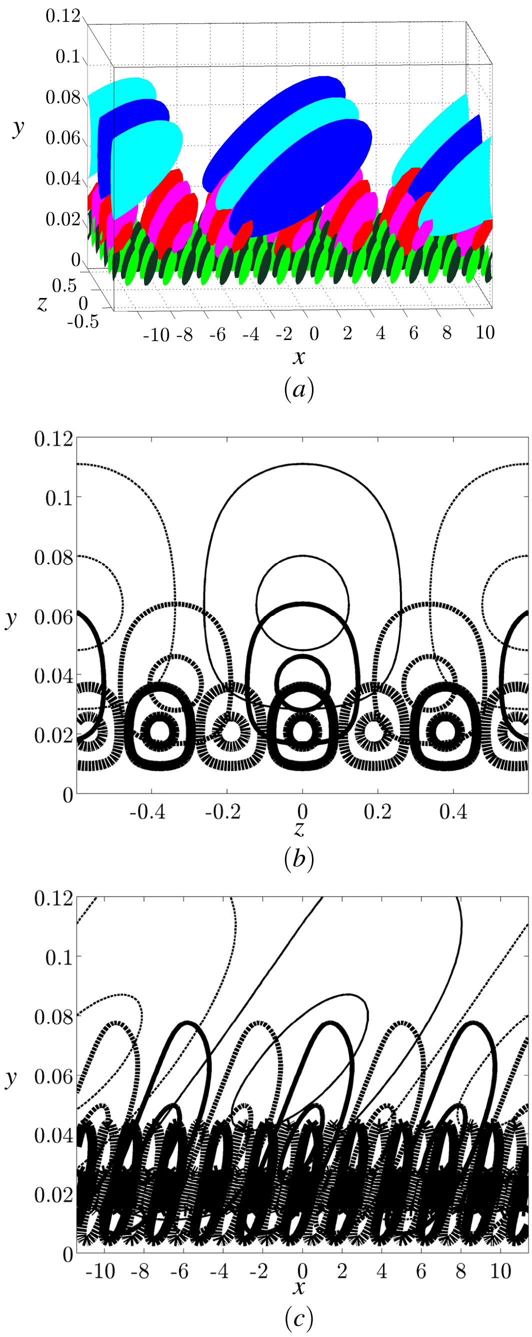


Figure 3. (a) The isosurfaces of the principal streamwise velocity corresponding to the modes that belong to the same hierarchy: $(\lambda_x, \lambda_z, c) = (2.3, 0.38, 17.35)$, blue; $(7.2, 0.67, 18.70)$, red; and $(72.1, 2.1, 20.05)$, green. The dark and light colors show 70 and $-70$ percent of the maximum velocity, respectively. The contours in (b) and (c) show cross-sections of (a) for $x = 0$ and $z = 0$ where thicker curves correspond to smaller modes. The positive (solid) and negative (dashed) contours represent $\pm 20$ and $\pm 80$ percent of the maximum velocity.

## CONCLUDING REMARKS

We illustrate that geometrically self-similar modes are inherent features of the NSE in the presence of a logarithmic mean velocity. It was shown that the logarithmic mean velocity, the criticality of singular modes, and the balance between viscous dissipation and mean advection terms in the resolvent represent necessary and sufficient conditions for the linear sub-units in the NSE to admit self-similar modes whose length and width respectively scale quadratically and linearly with their height. The wall-normal length scale is inherited from the turbulent mean velocity, and the wall-parallel length scales are determined from the balance between the viscous dissipation term, $(1/Re_\tau)\Delta$, and the mean advection terms, e.g. $\mathrm{i}\kappa_x(U - c)$. In addition, since the nonlinear terms determine the coefficients of the response modes corresponding to the linear sub-units, we argue that the above-mentioned conditions are also necessary for self-similarity in real turbulent flows; determining the sufficient conditions is a topic of ongoing research.

The identified scalings enable analytical developments in the overlap ('logarithmic') region of the turbulent mean velocity and result in significant simplifications in analysis of wall turbulence. An outgrowth of our recent efforts (Moarref *et al.*, 2013), the proposed analysis can be used to effectively bridge the gap between the inner and outer regions of the streamwise energy density and enable its scaling to arbitrary large Reynolds numbers. In addition, the wall-normal locality of the self-similar modes in a given hierarchy suggests that the linear sub-units in the NSE impose a direct correspondence between wall-parallel scales and wall-normal locations in the 'logarithmic' region. In the classical cascade analogy, this is reminiscent of an inertial regime studying of which is a topic of ongoing research. Furthermore, the identified scalings are expected to yield better understanding of the structure and evolution of the hypothesized attached eddies.

## ACKNOWLEDGEMENTS

The support of Air Force Office of Scientific Research under grants FA 9550-09-1-0701 (P.M. John Schmisseur) and FA 9550-12-1-0469 (P.M. Doug Smith) is gratefully acknowledged.

## REFERENCES

Hwang, Y. & Cossu, C. 2010 Linear non-normal energy amplification of harmonic and stochastic forcing in the turbulent channel flow. *J. Fluid Mech.* **664**, 51–73.

Marusic, I., Monty, J. P., Hultmark, M. & Smits, A. J. 2013 On the logarithmic region in wall turbulence. *J. Fluid Mech.* **716**, R3–1 – 716 R3–11.

McKeon, B. J. & Sharma, A. S. 2010 A critical-layer framework for turbulent pipe flow. *J. Fluid Mech.* **658**, 336–382.

McKeon, B. J., Sharma, A. S. & Jacobi, I. 2013 Experimental manipulation of wall turbulence: A systems approach. *Phys. Fluids* **25**, 031301.

Moarref, R., Sharma, A.S., Tropp, J.A. & McKeon, B.J. 2013 Model-based scaling and prediction of the streamwise energy intensity in high-Reynolds number turbulent channels. *J. Fluid Mech.* Submitted, also: `http://arxiv.org/pdf/1302.1594`.

Perry, A. E. & Chong, M. S. 1982 On the mechanism of wall turbulence. *J. Fluid Mech.* **119** (173), 106–121.

Smits, A. J., McKeon, B. J. & Marusic, I. 2011 High-Reynolds number wall turbulence. *Annu. Rev. Fluid Mech.* **43**, 353–375.

Townsend, A. 1976 *The structure of turbulent shear flow*. Cambridge University Press.

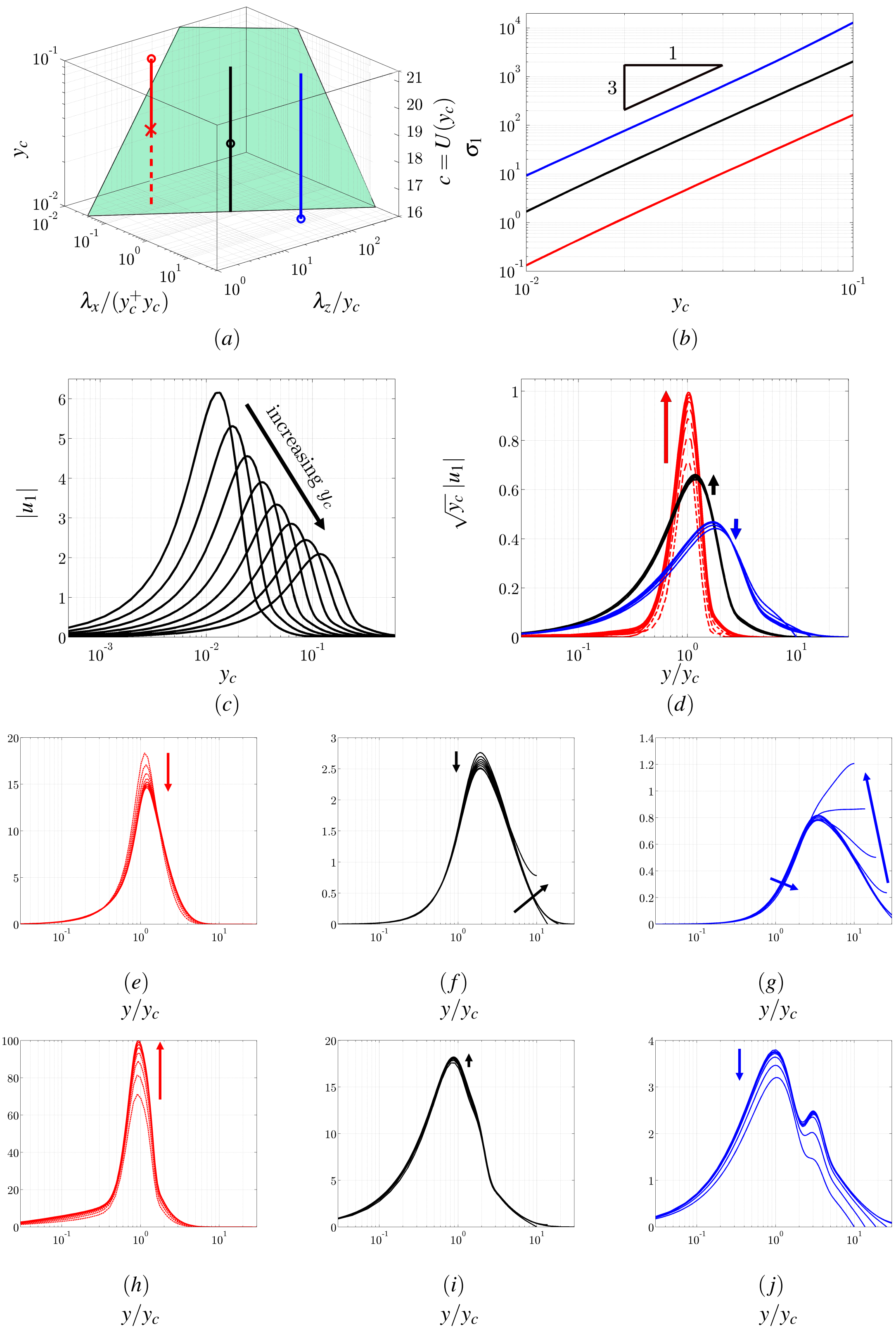


Figure 4. (a) The vertical lines are the loci of wave parameters that belong to the hierarchies with representative modes (open circles) $\kappa_{x,r} = 1$, $\kappa_{z,r} = 10$, and $c_r = 16$ (blue), $(2/3)U_{cl}$ (black), and $U_{cl} - 6.15$ (red) for $Re_\tau = 10000$. The shaded threshold plane corresponds to the wavenumbers with aspect ratio $\lambda_x/\lambda_z = \sqrt{10}$. The modes below this plane do not belong to any hierarchy. (b) The principal singular values along the hierarchies in figure 4(a). (c) The principal streamwise singular functions for the modes that belong to the hierarchy with $c_r = (2/3)U_{cl}$ in figure 4(a). (d)-(j) The normalized and scaled (according to table 1) principal streamwise, (d), wall-normal, (e)-(g), and spanwise, (h)-(j), singular functions for the modes along the hierarchies in figure 4(a). The arrows show the direction of increasing $y_c$ with $100/Re_\tau \le y_c \le 0.1$.